



## Influence of Imperfections in FEM Modeling of Lateral Torsional Buckling

N. Boissonnade<sup>1</sup>, H. Somja<sup>2</sup>

### Abstract

Present paper deals with the numerical modeling of the lateral torsional buckling phenomenon of rolled or welded steel profiles. More precisely, the definition of initial imperfections is of concern, the aim being here to investigate the influence of both geometrical and material imperfections on the bending resistance of such members. In this respect, present developments investigate the influences of several initial imperfections that are usually taken into account in FEM shell-modeling: stress-strain relationship, residual stresses, weak axis initial imperfection, initial torsional twist, local plate imperfections... The results of hundreds of GMNIA<sup>3</sup> calculations are reported, and the influences of these parameters on the carrying capacity are compared. Finally, recommendations for FE-modeling are given.

### 1. Introduction – Motivation

Present paper deals with the use of finite element models to simulate the behavior of members with respect to the Lateral Torsional Buckling (LTB) phenomenon. In particular, FE-modeling by means of *shell* elements is of concern. Indeed, the development of calculation software and pre and post-processors (e.g. meshing tools) in the last two decades has been such that resorting to FEM-shell models to investigate LTB or other structural phenomena has become a “standard” practice. Still, the numerical models need to be validated, preferably towards test results.

The latter step however reveals to be quite delicate to perform, especially in terms of load application and practical support conditions (so-called “fork conditions”); in addition, experimental tests usually require significant amounts of time and money. Then, even if this “validation step” is crucial, temptation to resort solely to numerical tools is important, since, further to being considerably faster and economical, they allow for an effective gathering of reference results. Moreover, it becomes possible to isolate the influence of a single parameter (e.g. influence of the beam length), which, from a scientific point of view, goes without comparison.

In this context, information on initial imperfections to be considered in the numerical computations appears to be a key aspect, namely concerning the geometrical ones. Further, the definition of “standard” initial imperfection sets within parametric studies is decisive.

---

<sup>1</sup> Professor, University of Applied Sciences of Western Switzerland, <nicolas.boissonnade@hefr.ch>

<sup>2</sup> Associate Professor, National Institute of Applied Sciences of Rennes, <hugues.somja@insa-rennes.fr>

<sup>3</sup> GMNIA: Geometrically and Materially Non-linear with Imperfection Analysis

If such information seems to be well recognized and worldwide-accepted for flexural buckling (Beer 1970), scarce and misleading recommendations are available in the literature for the particular case of LTB, where one may find as much choices for initial imperfections as authors or researchers who studied LTB from a numerical point of view. One may cite in a non-exhaustive manner the works of Ofner (1997), Greiner (2000), RFCS (2002), Silva (2007), Talamona (2008), Knobloch (2008), Mendonça (2008), Kindman (2011)...

As a consequence, it becomes almost impossible to accurately compare and/or validate results between authors, nor to clearly define which types of imperfections and their corresponding amplitudes should be considered in FEM calculations.

In order to contribute filling this lack of guidance, present paper intends at providing information on the FEM modeling of the most relevant imperfections, i.e. those having a potential influence on the carrying capacity of steel members towards LTB. Section 2 first describes the FEM shell models that have been used as a basis for present study; Section 3 then focuses on the influence of residual stresses distributions, while Section 4 deals with various initial geometrical imperfection patterns. Finally, Section 5 proposes practical recommendations for a sound introduction of imperfections in the modeling of LTB.

## 2. Description of FEM models – Modeling of imperfections

### 2.1 FEM (shell) models

Extensive series of numerical computations have been led with the use of non-linear FEM software FINELg (2012), continuously developed at the University of Liège and Greisch Engineering Office since 1970. This software offers almost all types of FEM types of analyses, and present investigations have mainly been resorting to so-called MNA (Materially Non-linear Analysis), LBA (Local Buckling Analysis) and GMNIA analyses. Use of quadrangular 4-nodes plate-shell finite elements with typical features (Corotational total Lagrangian formulation, Kirchhoff's theory for bending) has been made. Density and quality of the different meshes used here has been preliminarily assessed, and several modeling specificities are further described below.

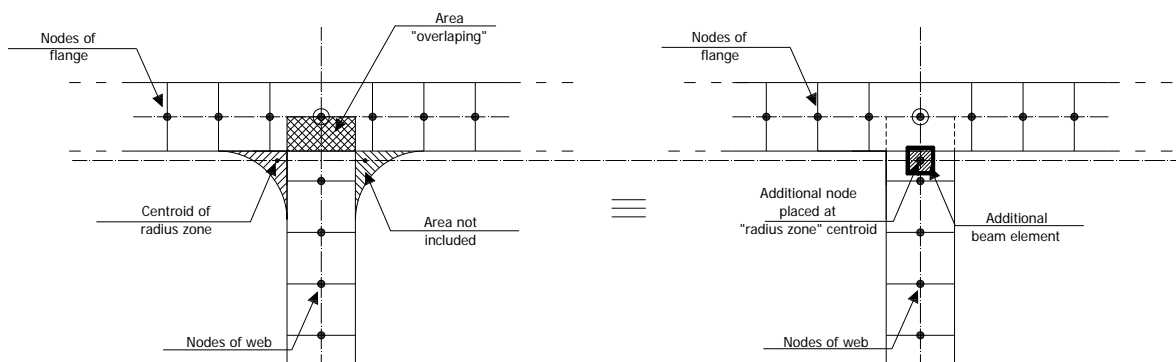


Figure 1: FEM-treatment of web-to-flange junction

First, the web-to-flange zone has been receiving a specific treatment (see Fig. 1). Within shell modeling, this region indeed suffers from i) an overlap of material, and from ii) the disregarding of so-called “flange radius” areas. In order to get closer to the real characteristics of such steel cross-sections, an additional node has been placed within the web height, at the exact vertical position of the centroid of the radius zone. In addition to being linked with the elements of the

web, this node bears an additional beam element, oriented in the  $x$  direction, whose (square) cross-section area is equal to that of the radius zones minus the overlapped area. This extra beam element allows for nearly-exact cross-sectional properties of the shell element in comparison to analytical (catalogue) ones; it is also given the same constitutive law as the one of the plate elements.

In terms of support conditions, two main aspects have been distinguished for the definition of the reference “fork conditions” at the member’s ends. The first one concerns the treatment of in-plane cross-sectional local supports. These have been defined as Fig. 2a shows, and consequently provide i) *local* lateral support to possible local buckling owing to concentrated support reactions, as well as ii) *global* cross-section fork condition supports, namely lateral and vertical deflections, as well as torsional twist.

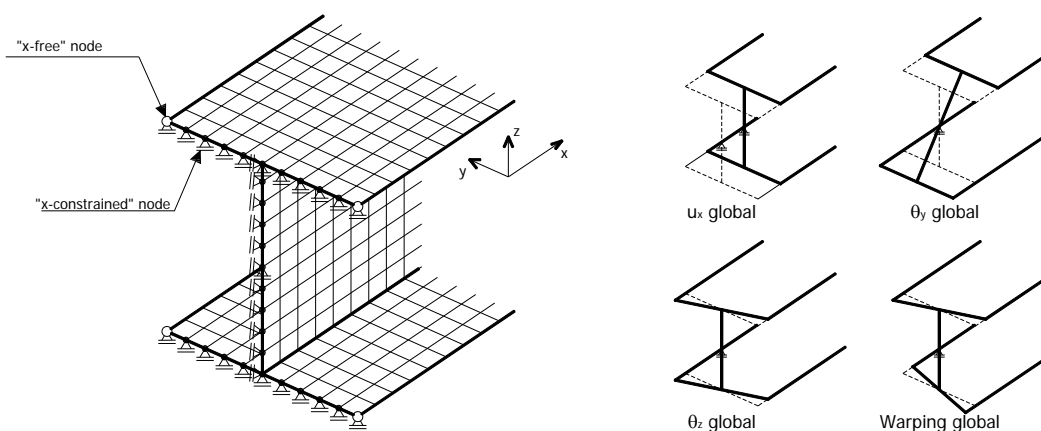


Figure 2: Support conditions

The second aspect deals with the possible axial displacements (“ $x$ -oriented”) of the end cross-section nodes. In order to allow for a maximum number of four *global* degrees-of-freedom of the end cross-section (i.e. axial displacement, rotations  $\theta_y$ ,  $\theta_z$  and warping), use of linear constraints has been made between the flange and web nodes. While a maximum of four nodes may experience a “free” longitudinal displacement, all other nodes’  $x$ -displacements linearly depend on the longitudinal displacements of the “ $x$ -free” nodes to respect a *global* cross-sectional displaced configuration, as Fig. 2b shows.

For sake of symmetry, the four nodes at the flanges tips have been chosen as the “ $x$ -free” ones, and all other nodes are consequently the “ $x$ -constrained” ones. Doing so allows for a sufficiently correct treatment of the global cross-section behavior, given the usual levels of displacements and rotations reached within present study. It also avoids the usual technique of superposing additional stiff elements along the flanges and webs of the end-sections (Semi-Comp 2007) that aim at preventing local instabilities but may generate numerical troubles. This modeling technique has been shown to be very effective from a numerical point of view (Semi-Comp 2007), and was validated and adopted in many FEM studies.

The application of any external loading at the member’s ends (i.e. strong and weak axis bending moments and/or axial forces) is straightforward, and has been implemented by means of suitable distributions of concentrated forces at the flanges tips, see Fig. 3a. As a further feature of the adopted linear constraints relationships, this way of introducing end forces is seen to avoid any unintended stress concentrations, see Fig 3b.

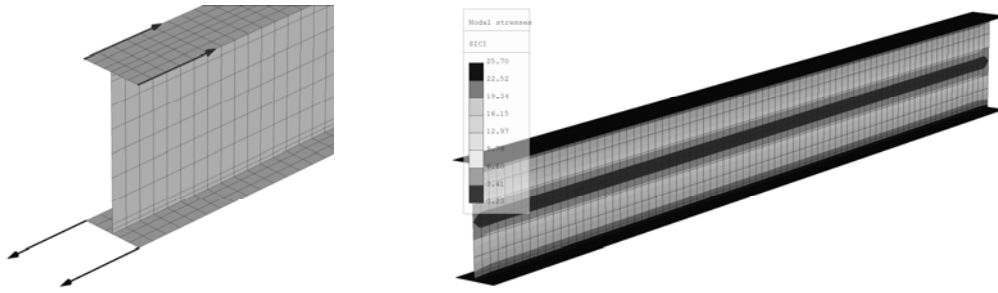


Figure 3: a) Applied loads at flanges tips b) Isolines of stresses under major axis constant bending moment

## 2.2 Modeling of material imperfections and strain-hardening

Material imperfections have been accounted for by means of so-called “residual stresses” distributions. These “membrane” stresses are indeed known to have an influence on the carrying capacity of beams in an LTB failure mode, and several patterns have been studied and compared (Fig. 4).

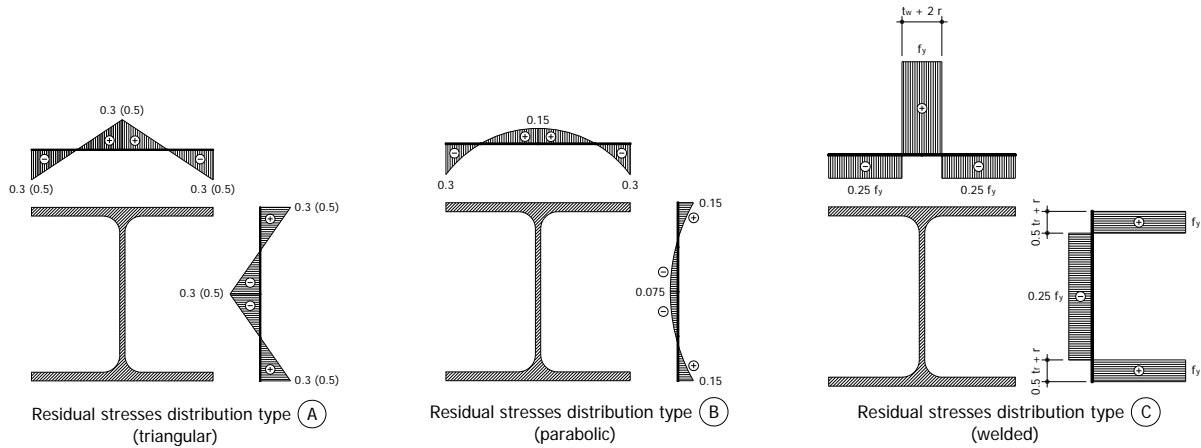


Figure 4: Possible residual stresses distributions

An important number of “standard” residual stresses distributions may be found in the literature (Tebedge 1973, Grimault 1985, DIN 1990). As an example, the triangular distribution “type A” may be proposed with a maximum residual stress equal to either  $0.3 f_y$  (IPE sections) or to  $0.5 f_y$  (HE-shapes), depending on the dimensions of the cross-section.

Basically, 3 different types of distributions have been considered here, so-called triangular, parabolic and welded types. They are defined so that the various stresses distributions are in auto-equilibrium, preferably within each plate.

In addition to various distributions of stresses along the cross-section, the particular cases of triangular and parabolic distributions may refer to either the actual yield stress  $f_y$  or to a reference  $f_y^* = 235 \text{ N/mm}^2$  one. This aspect is studied in more detail in Section 3.

The  $\sigma - \varepsilon$  constitutive laws adopted herein have consisted in one of the 3 distributions of Fig. 5. These are frequently used in numerical studies, and are generally assumed to represent the actual behavior of structural steel in a suitable way. In order to refer to a single  $\sigma - \varepsilon$  curve in the following, the influence of each constitutive law on the LTB response of IPE 500 and HEB 300 members has been investigated, and results are presented in Figs. 6a and 6b.

“Standard” LTB situations have been considered here, i.e. constant applied bending moment and fork end conditions.

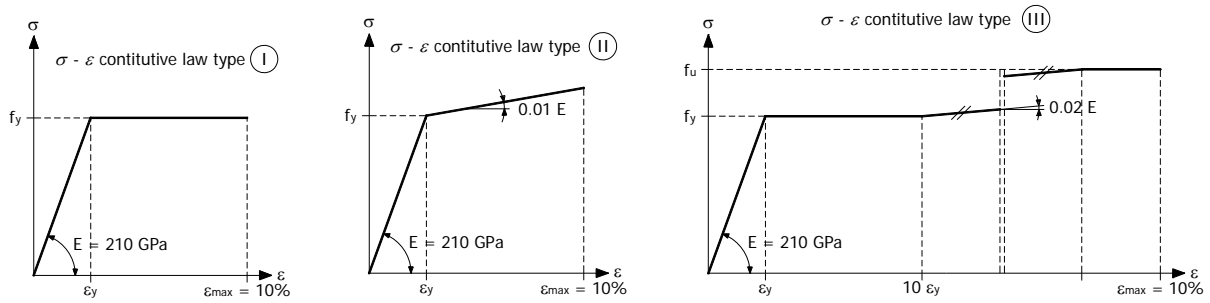


Figure 5: Investigated  $\sigma - \varepsilon$  stress-strain laws

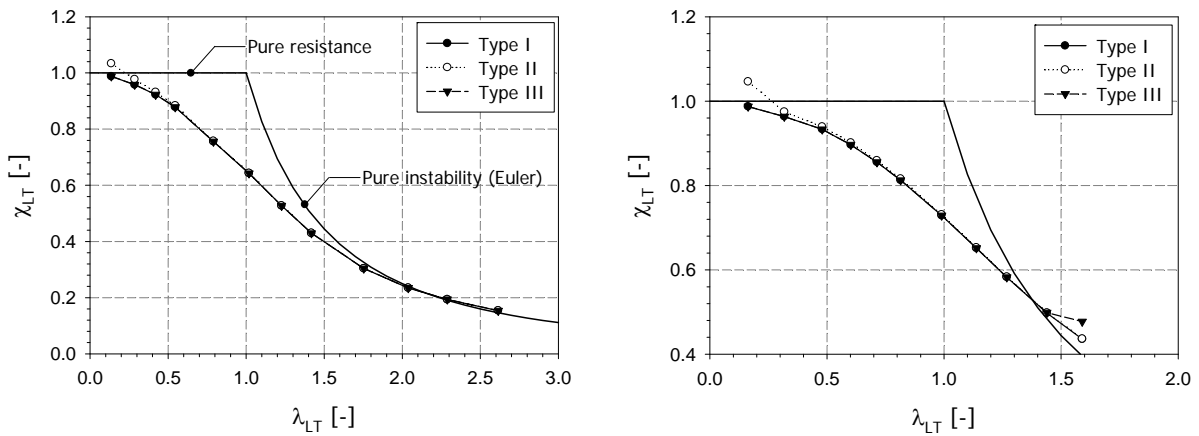


Figure 6: Influence of stress-strain law – a) IPE 500 – b) HEB 300 (S355 steel)

Figs. 6a and 6b, as well as many of the figures following, plot the obtained numerical results in terms of  $\chi_{LT} - \lambda_{LT}$  curves, where  $\lambda_{LT}$  is defined as the relative slenderness to LTB  $\lambda_{LT} = (M_{Rk} / M_{cr})^{0.5}$ ,  $M_{Rk}$  and  $M_{cr}$  being the strong axis pure bending resistance and the elastic critical bending moment, respectively.  $\chi_{LT}$  is defined so that the ultimate bending moment  $M_{ult} = \chi_{LT} M_{Rk}$ , i.e.  $\chi_{LT}$  can be interpreted as a “penalty” on the pure cross-section resistance owing to instability effects.

As can be seen, the differences between the curves appear to be systematically negligible, except for very stocky (short) members where strain-hardening is seen to have an influence. However, in such situations the member is so short that it can hardly still be considered as a *beam* member. Therefore,  $\sigma - \varepsilon$  “type III” (i.e. elastic – plateau – strain-hardening) has been kept in the following FEM computations.

It shall also be noticed that for some high  $\lambda_{LT}$  values, the FEM curves may “cross” the Euler curve; this may be explained by the fact that i) for such long members, the observed levels of curvature are such that the assumptions of the Euler curves (namely small rotations) may no longer be fulfilled, and ii) because the corresponding profiles partially mobilize weak axis resistance, the weakest cross-section being almost rotated  $90^\circ$  about the x-axis. This influence is even more observed for the HEB section since its relative weak axis resistance  $M_{z,Rk}$  is greater than for the IPE section.

It may be noted that Figs. 6a and 6b also refer to the following set of initial imperfections:

- Residual stresses: parabolic distributions + reference to  $f_y^*$  values;
- Geometrical imperfections: “type 1” + no local imperfections (see § 2.3).

This specific combination of imperfections has been established as a reference set of initial imperfections and is frequently referred to in the following.

### 2.3 Modeling of geometrical imperfections

Initial geometrical imperfections have been basically introduced through adequate modifications of node coordinates, i.e. the initial geometry slightly differs from the ideal one. Both *global* and *local* imperfections have been taken into account; global initial geometrical imperfections usually consist in the superposition of i) a weak axis (lateral) initial default and of ii) an initial torsional twist, see Fig. 7. They both vary sinusoidally from zero at the member’s ends to a maximum at mid-span, and each amplitude can be set independently. Alternatively, the combined global imperfection may be seen as the one obtained through adequate lateral displacements of both the top and bottom flanges, see Table 1.

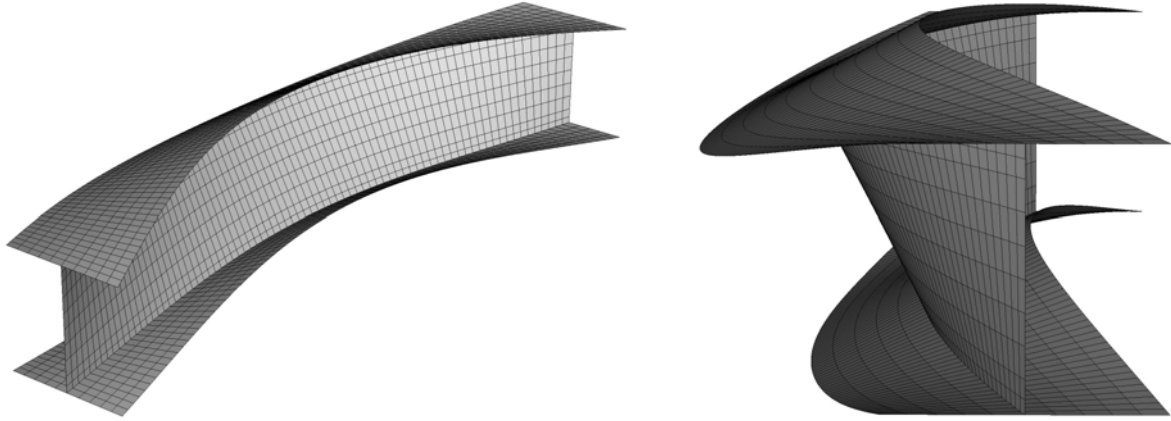


Figure 7: Global imperfections (magnified)

In the following, several combinations and amplitudes have been investigated, and are schematically represented by Figs. 13, 15 and 17. Table 1 also summarizes the various amplitudes studied.

Table 1: Definitions of initial global geometrical imperfections

Geom. imperf. type	$\Delta_{\text{lat. global}}^1$	$\psi_{\text{ini}}^1$	$\Delta_{\text{lat. top flange}}$	$\Delta_{\text{lat. bottom flange}}$
1	$L / 1\,500$	$L / (2\,000 h)$	$11 L / 12\,000$	$5 L / 12\,000$
2	$L / 1\,000$	0	$L / 1\,000$	$L / 1\,000$
3	0	$L / (1\,000 h)$	$L / 2\,000$	$-L / 2\,000$
4	$L / 1\,500$	$4 L / (1\,500 h)$	$L / 500$	$-L / 1\,500$
5	$L / 2\,000$	$L / (2\,000 h)$	$3 L / 4\,000$	$L / 4\,000$
6	$L / 1\,000$	$L / (2\,000 h)$	$5 L / 4\,000$	$3 L / 4\,000$
7	$L / 500$	$L / (2\,000 h)$	$9 L / 4\,000$	$7 L / 4\,000$
8	$L / 4\,000$	$L / (2\,000 h)$	$L / 2\,000$	0
9	$L / 2\,000$	0	$L / 2\,000$	$L / 2\,000$
10	$L / 1\,500$	$-L / (2\,000 h)$	$L / 4\,000$	$3 L / 1\,000$
11	$L / 1\,000$	$-L / (1\,000 h)$	$L / 2\,000$	$3 L / 2\,000$

1.  $\Delta_{\text{lat}}$  stands for initial (lateral) imperfection, and  $\psi_{\text{ini}}$  for the initial torsional twist

Besides *global* “member” defaults, initial *local* geometrical imperfections may be taken into account, again by means of modified node coordinates. They shall allow for the potential influence of local instabilities on the member’s behavior, and are defined with analogy to plate instability modes, i.e. with a combination of sinusoidal “half-waves” in both directions of the considered plate. For both web and flanges, square half-wave patterns have been introduced with an amplitude of  $a/400$ , where  $a$  stands for the length of the considered “square” panel (see Eurocode 3 Part 1.5 “Plates” Annex C (CEN 2005)).

It is to be noted that, again, the definition of the local imperfections in the web is fully independent from that of the flanges: depending on the cross-section dimensions, a flange may be “buckled” in a considerably different configuration from that of a web, in terms of both amplitude and “wavelength”. Finally, local imperfections have been defined so that they do not affect the web-to-flange region, which is assumed to remain unaffected by initial geometrical imperfections and rigid, even in cases where local buckling occurs.

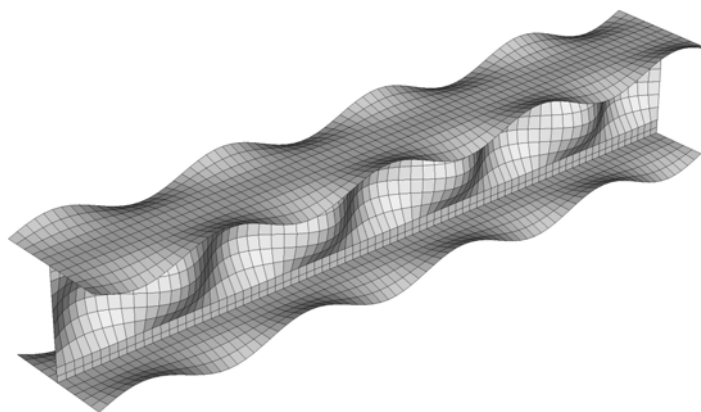


Figure 8: Local imperfections (magnified)

### 3. Influence of residual stresses distribution

#### 3.1 Residual stresses patterns

Present paragraph investigates the influence of the distribution of residual stresses on the carrying capacity of steel beams towards LTB. Figs. 9a and 9b present the obtained results, for various residual stresses patterns on an IPE 500 and on an HEB 300, respectively.

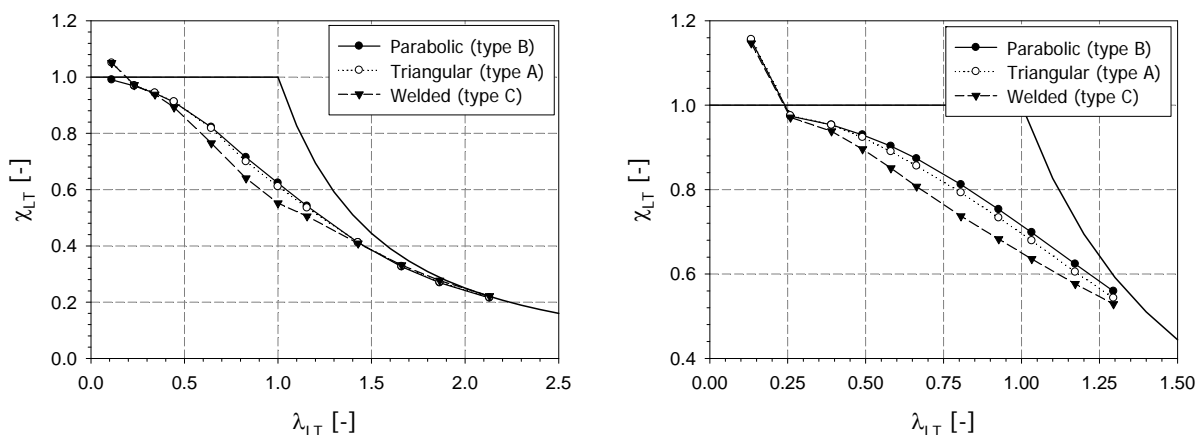


Figure 9: Influence of residual stresses pattern – a) IPE 500 – b) HEB 300

Again, reference is made to an elastic – plateau – strain-hardening constitutive law (“type III” with  $f_y = 355 \text{ N/mm}^2$ , see Fig. 5), with “type 1” geometrical imperfection and no local imperfections. Further, triangular (“type A”) and parabolic (“type B”) distributions refer to residual stresses distributions with respect to a conventional yield stress of  $235 \text{ N/mm}^2$ , while the “welded” (“type C”) distribution obviously refers to the actual yield stress, within the zones thermally affected by welding.

As can be seen, few differences between the triangular and parabolic distributions appear, unlike for the welded distribution. This typical behavior has been reported by other authors, through both beam and shell element modeling (Lam 2002, Greiner 2000), even with more complex and “accurate” distributions of the welded residual stresses. The differences are however worth 13%, which appear to be non-negligible. Fig. 10 also proposes the results corresponding to a member under fork conditions acted by a single-sided end moment (i.e. triangular bending moment distribution along the member, load case B), where the same tendencies may be observed.

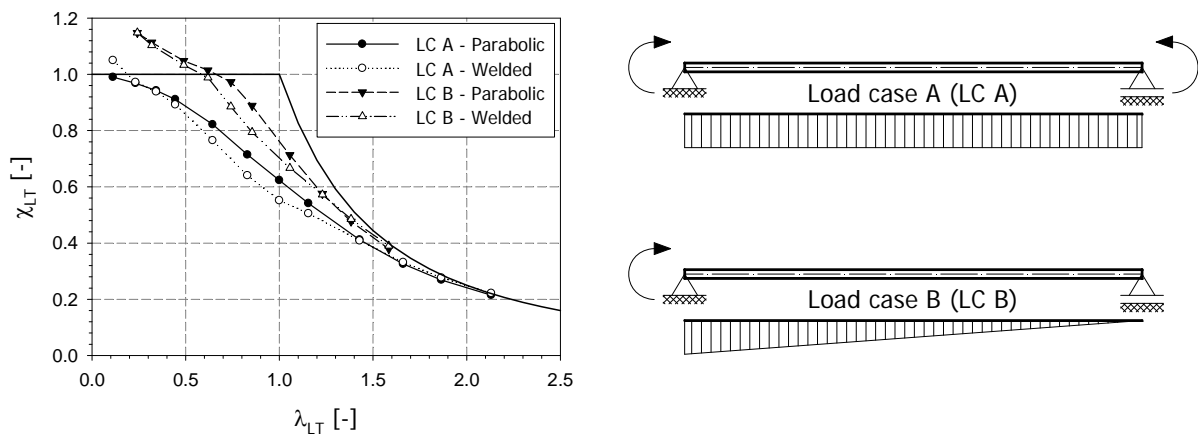


Figure 10: Influence of residual stresses pattern and bending moment distribution

Finally, Fig. 11 proposes a magnified view of the deformed shape of the FEM mesh once the sole parabolic residual stresses have been accounted for, i.e. prior to the application of any bending action. It can be seen that the resulting effect is similar to the application of a tension normal force, however of very low value, as a result of auto-equilibrated stresses.

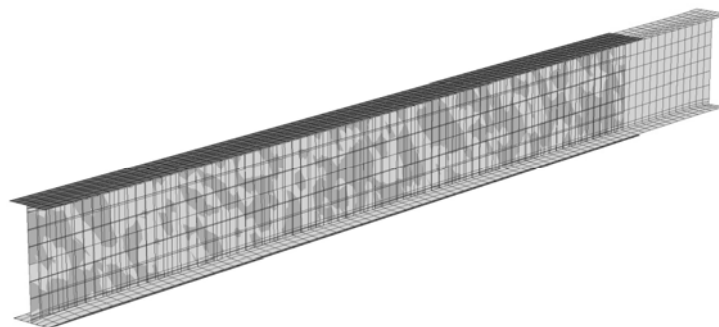


Figure 11: Deformed shape after numerical auto-equilibrium procedure (IPE 500, amplified 500 million times)

### 3.2 Influence of yield stress

As a complement to previous paragraph, present section relates to the yield stress to be referred to within the adopted distribution of residual stresses. As already explained, unlike the “welded”



situation which obviously refers to the actual yield stress  $f_y$ , the triangular and parabolic distributions may be found in the literature to be relative to either the *actual*  $f_y$ , or to a *reference*  $f_y^* = 235 \text{ N/mm}^2$  one. Figs. 12a to 12d show the obtained results, for steel grades S235, S355, S460 and S690, respectively.

First, the different figures confirm the expected penalizing influence of a welded residual stresses distribution, whatever the yield stress. Second, the influence of referring to the actual yield stress for the parabolic (or triangular) distributions is seen to be non-negligible, obviously for high steel grades. The divergence “measured” on these curves between a  $f_y^*$  and a  $f_y$  reference value for the residual stresses distributions may reach 8%. Hence, a decision to consider a reference to  $f_y$  or  $f_y^*$  clearly has to be made. According to experimental results within this field, it appears that preference should be given to  $f_y^*$ .

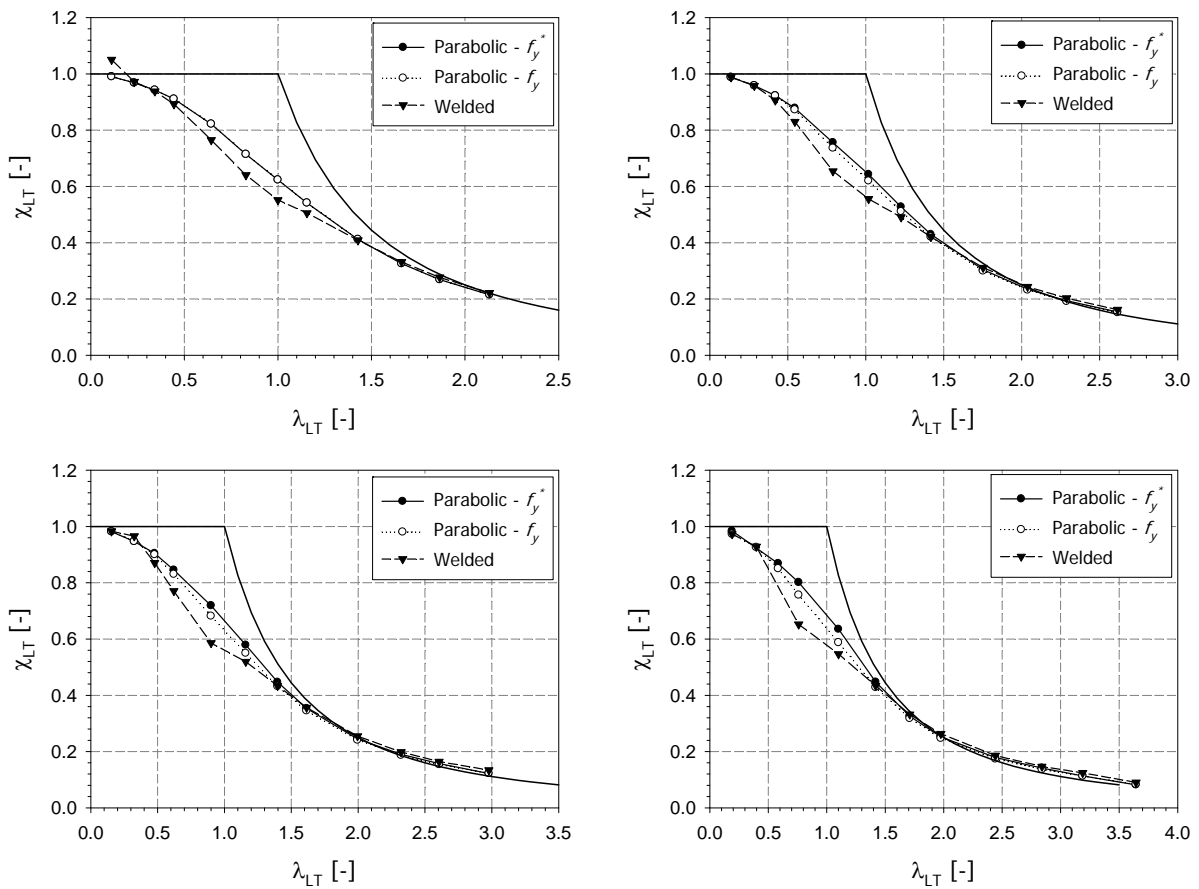


Figure 12: Influence of yield stress  $f_y$  on IPE 500 cross-section – a) S235 – b) S355 – c) S460 – d) S690

## 4. Influence of geometrical imperfections

### 4.1 Weak axis imperfection

This paragraph is devoted to the influence of the lateral (weak axis) initial geometrical imperfection on the member’s response to LTB. All the following results show how several initial amplitudes of the weak axis default may affect the bending resistance of the steel girder. Common features of the presented results are, again:

- Constant bending moment distribution along the member;

- Parabolic residual stresses distributions, with respect to  $f_y^*$ ;
- $f_y = 355 \text{ N/mm}^2$ ;
- Constant initial torsional twist equal to  $L / (2000 h)$ , see Table 1;
- No local geometrical imperfections.

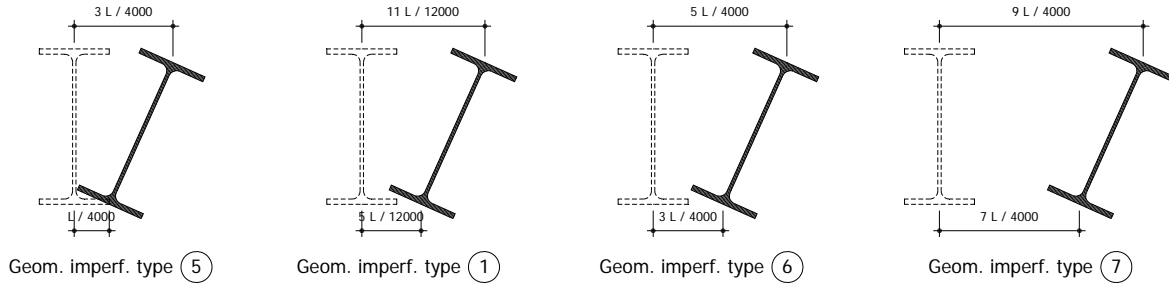


Figure 13: Designation for initial geometrical imperfection shape type

Figs. 14a and 14b below are relative to geometrical imperfections types 5, 1, 6 and 7 (see Fig. 13). As can be seen, “reasonable”<sup>4</sup> lateral imperfections, i.e. from  $L / 2000$  to  $L / 1000$ , cause little differences on the observed resistance. However, a  $L / 500$  amplitude drops the  $L / 1000$  resistance down to 10% in the worst cases; this situation is however usually outside fabrication tolerances, and may not be considered. Therefore, a realistic amplitude of the initial lateral default should lead to satisfactory results, given “standard” sets of imperfections (initial torsional twist, residual stresses).

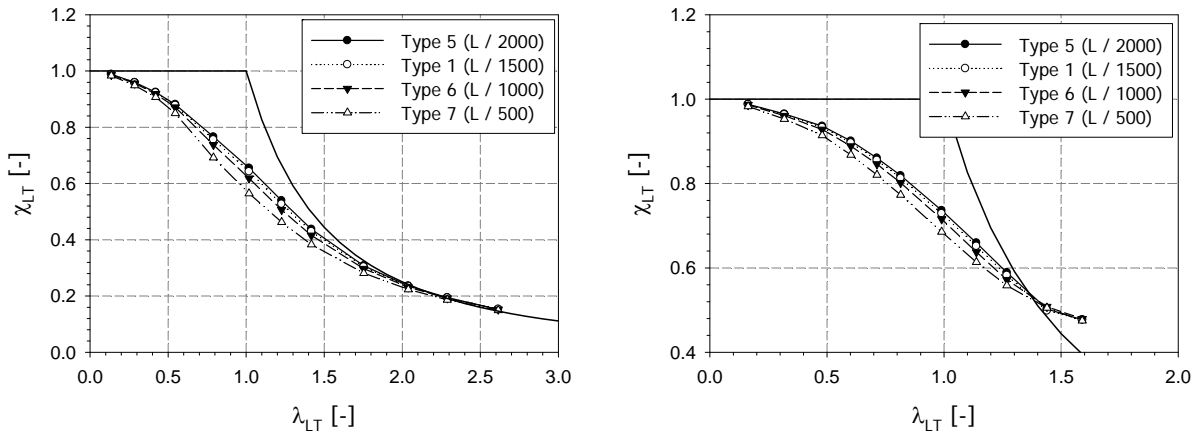


Figure 14: Influence of weak axis imperfection – a) IPE 500 – b) HEB 300

#### 4.2 Initial torsional twist

The second “geometrical” parameter that has been investigated is the amplitude of the initial torsional twist. Obviously, since the phenomenon of LTB generates x-axis torsional rotations, an initial torsional twist ought to be considered, with amplitude to be defined. Fig. 15 lists a series of initial torsional twists accounted for in the FEM simulations, from zero to  $4 L / (1500 h)$  (see also Table 1).

Figs. 16a and 16b plot the obtained results, for the reference case of constant bending moment and fork support conditions, on a S355 member with a parabolic residual stresses distribution.

<sup>4</sup> Experimental measurements show that within Europe’s production, a realistic average value of steel member’s initial bow imperfection amplitude lies around  $L / 1000$ , where  $L$  is the length of the member.

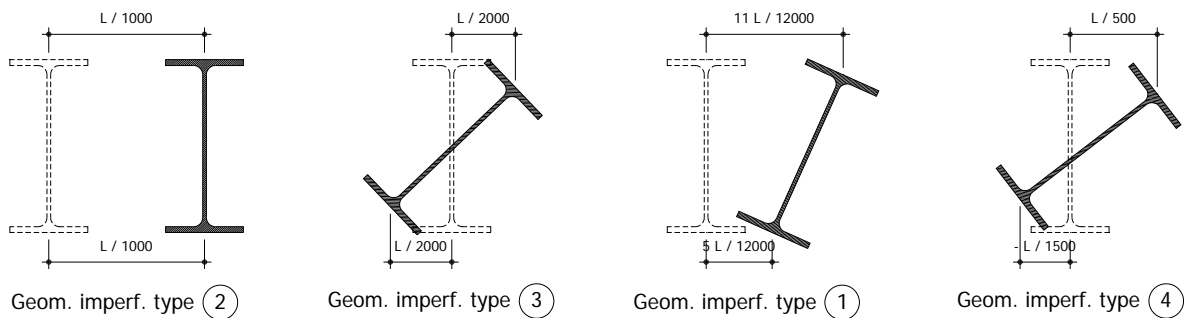


Figure 15: Designation for initial geometrical imperfection shape type

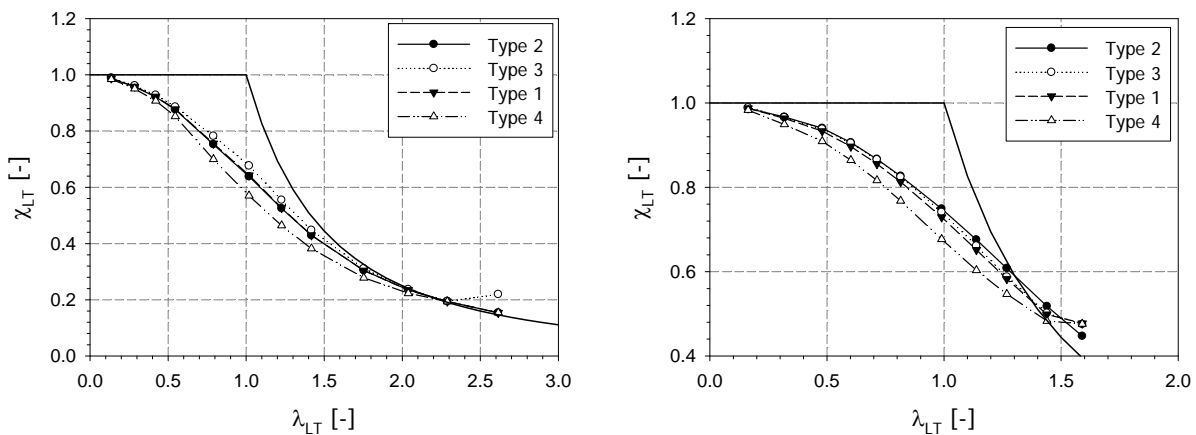


Figure 16: Influence of initial torsional twist – a) IPE 500 – b) HEB 300

As can be seen, except for the (unrealistic) case of “type 4” geometrical imperfection pattern, all results are very close, for the IPE 500 profile as well as for the HEB 300. This indicates that reasonable amplitudes for the initial torsional twist may be seen as adequate to initiate the phenomenon. Further, a comparison between reasonable geometrical imperfection patterns “type 2” (no initial torsional twist) and “type 3” (no initial global cross-sectional weak axis default) shows that the influence of the lateral geometrical imperfection has probably more influence than an initial torsional twist. A combination of both geometrical defaults is then seen to be the most appropriate.

#### 4.3 Tension flange imperfection

Present paragraph focuses on the initial lateral imperfection given to the *tension* flange, i.e. on its influence (amplitude of global cross-section lateral default + initial torsional twist) on the carrying capacity towards LTB.

This focus may appear somehow surprising, since it would at first be expected that the imperfection given to the (upper) flange in *compression* rules the member’s behavior. It has however been sometimes suggested (Villette 2004) that the imperfection given to the tension flange might be a leading parameter on the resistance to LTB.

Therefore, Fig. 17 sets of imperfections have been investigated, and Figs. 18a and 18b present the obtained results, for an IPE 500 and an HEB 300 cross-section, respectively. As can be seen, in the particular case of the IPE 500 section, the differences between the various curves are negligible. However, the HEB 300 results show a 10% difference for slenderness values greater

than 1.0, in the way of a higher influence of the initial torsional twist, i.e. the initial lateral imperfection of the tension flange does not appear as a governing factor.

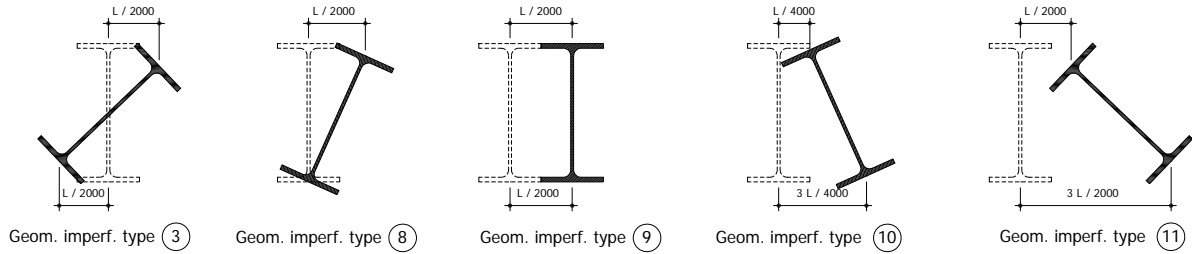


Figure 17: Designation for initial geometrical imperfection shape type

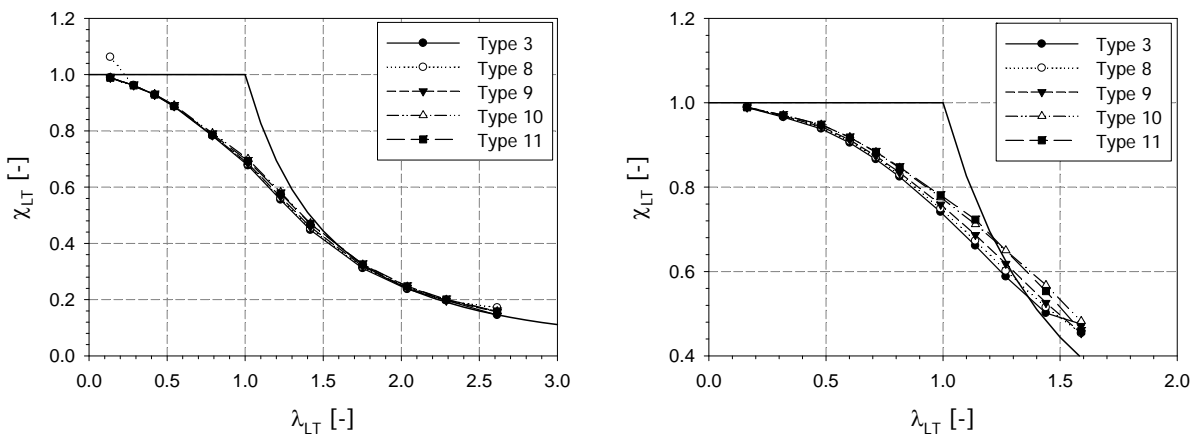


Figure 18: Influence of initial tension flange imperfection – a) IPE 500 – b) HEB 300

One may also notice that this influence is stronger for the HEB 300 cross-section, which is due to the fact that the weak axis resistance of the HEB 300 is relatively stronger than that of the IPE 500, thus the less important influence of the top flange imperfection.

#### 4.4 Influence of local imperfections

Figs. 19a and 19b below intend at investigating a possible influence of *local* geometrical imperfections. Reference is again made to S355 members with parabolic residual stresses and initial global geometrical imperfections according to “type 1” definition.

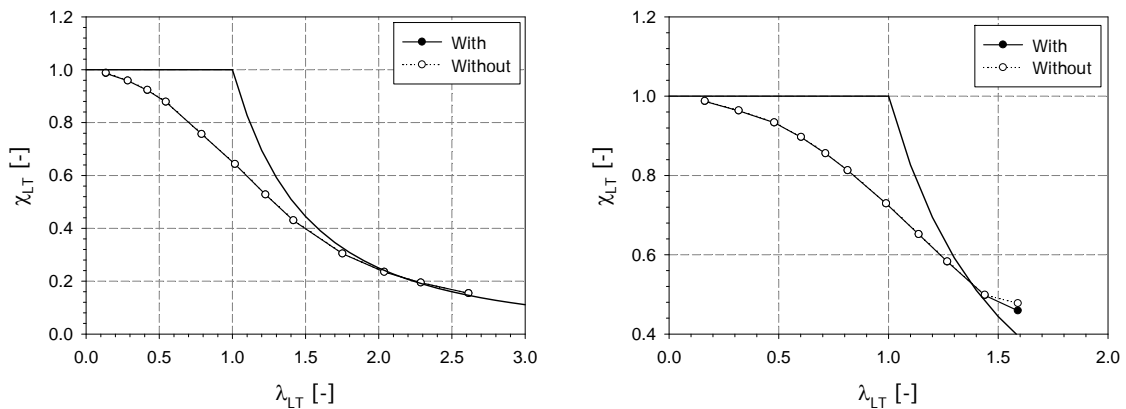


Figure 19: Influence of local imperfections – a) IPE 500 – b) HEB 300

As can be seen, the curves “with” and “without” local defaults are fully coincident, indicating that such initial imperfections may be “omitted” in the modeling; this is mainly justified by the fact that the investigated cross-sections do not comprise any highly slender component, so that the influence of local buckling on the global behavior remains negligible.

#### 4.5 Use of eigenmodes for the definition of the imperfect geometry

This final subsection deals with the use of LBA-obtained eigenmodes for the definition of the initially-imperfect geometry. For this purpose, relevant eigenmodes have been used to derive the initial geometrical imperfection. A “scale factor” of  $L / 1000$  has been used to set the top flange maximum lateral imperfection at mid-span. Figs. 20a and 20b report on the obtained results.

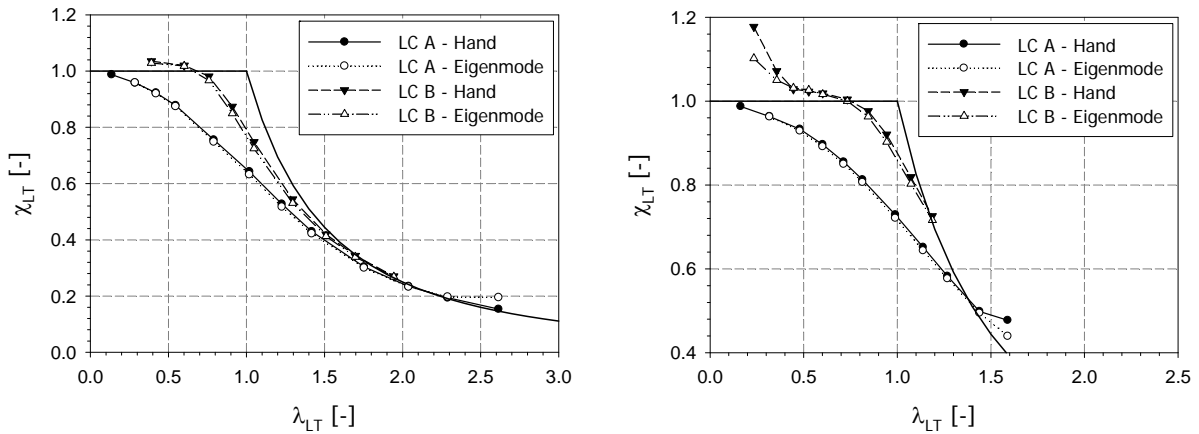


Figure 20: Effect of the use of eigenmodes for the geometrical imperfection shape – a) IPE 500 – b) HEB 300

As can be seen, the differences between the “hand-defined” and the “eigenmodes” curves are negligible for the constant bending moment situation (LC A). Little difference may however appear for load case B, for about 3%. This may be explained through the fact that the maximum initial lateral default of the “eigenmode” situation is no longer located at mid-span, unlike the one for the “hand-defined” situation that still is.

## 5. Recommendations for FEM modeling

As a summary of the performed investigations, the following features may be recommended for the modeling of LTB:

- No strain-hardening may be considered in the  $\sigma - \varepsilon$  law. This may be in contradiction with the recommendations proposed in the informative Annex C of Eurocode 3 Part 1.5 (CEN 2005);
- For rolled profiles, parabolic or triangular residual stresses patterns in auto-equilibrium along each individual plate are recommended, with a reference yield stress  $f_y^*$  equal to  $235 \text{ N/mm}^2$ ;
- No local geometrical imperfections are needed, provided that the different plates of the cross-section do not belong to the “slender” range (i.e. no “Class 4” elements);
- Combination of global cross-section lateral imperfection with initial torsional twist  $\psi_{ini}$  seems adequate, with reasonable amplitudes (“type 1” for example);
- Use of eigenmodes as initial imperfect shape is suitable, provided a careful scaling of the initial amplitude ( $L / 1000$  is recommended).

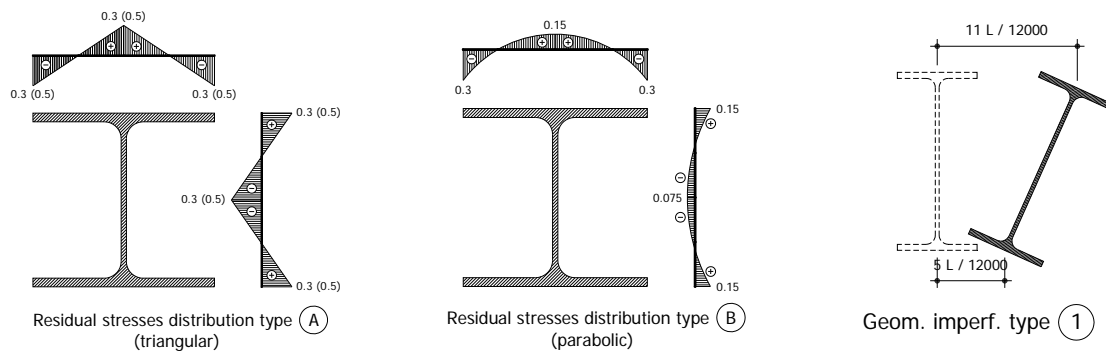


Figure 21: Recommended sets of initial imperfections

## 6. Conclusions

In this paper, investigations towards the influence of imperfections on the FEM modeling of the LTB phenomenon have been led. Typical influences of the constitutive law definition, of the residual stresses adopted distributions and of geometrical initial imperfections (both local and global) have been studied, through adequate shell models. More than 700 results of FEM simulations show that i) an adequate and reasonably realistic set of residual stresses, initial lateral imperfection and torsional twist lead to consistent results, and that ii) such “standard” definitions may be used in FEM-led parametric studies. Detailed recommendations for FE modeling (type and amplitudes) are also finally given.

## References

- Beer, H., Schulz, G. (1970). “Bases théoriques des courbes européennes de flambement.” *Construction Métallique*, n°3.
- CEN (Comité Européen de Normalisation) (2005). “Eurocode 3: Design of Steel Structures, Part 1–5: Design of plated structures (EN 1993 1-1)”, Brussels.
- DIN 18800 1-4: 1990 (1990). “Stahlbauten.” *Beuth Verlag GmbH*, Berlin.
- Greiner, R. et al. (2000). “Report – 18 April 2000”, *ECCS Report April 18<sup>th</sup>*.
- Greiner, R., Salzgeber, G., Ofner, R. (2000). “New lateral torsional buckling curves  $\chi_{LT}$  – Numerical simulations and design formulae”, *ECCS Report June 30<sup>th</sup>*.
- Grimault, J.P., Rondal, J. (1985) “Etude comparative de différentes méthodes de mesure des contraintes résiduelles dans les profils creux en acier.” *Paris and Liège*.
- Kindmann, R., Kraus, M. (2011). “Steel Structures – Design using FEM.” *Ernst&Sohn*.
- Knobloch, M., Fontana, M., Frangi, A. (2008). “Steel beam-columns subjected to fire.” *Proceedings of the 5<sup>th</sup> European Conference on Steel and Composite Structures*, Graz, Austria.
- Lam, L. (2002). “Comparative study of the verification of the instability in lateral torsional buckling formulae”, *Internal report*, University of Liège.
- “Lateral torsional buckling in steel and composite beams” (2002). *Final report – RFCS – Steel RTD (Contract 7210-PR-183)*.
- Mendonça, P., Camotim, D. (2008). “EC3 safety checking of compact I-section beam-columns.” *Proceedings of the 5<sup>th</sup> European Conference on Steel and Composite Structures*, Graz, Austria.
- Non-linear finite element analysis program “FINELg” (2012), *User’s Manual, version 9.3*, ArGenCo Department, University of Liège, Greisch Info S.A., Liège, Belgium.
- Ofner R. (1997) “Traglast von Stäben aus Stahl bei Druck und Biegung”. *PhD Thesis*, Graz Technical University.
- “Plastic member capacity of semi-compact steel sections – a more economic design (Semi-Comp)” (2007). *Final report (01/01/06 – 30/06/07) – RFCS – Steel RTD (Contract RFS-CR-04044)*.
- Silva, L.S. (2007). “Use of FEM in the design of steel Structures.” *ECCS Technical Committee 8 - Stability*, Doc. ECCS-TC8-2007-002.
- Talamona, D., Lopes, N., Vila Real, P., Castagne, S., Franssen, J.M. (2008). “Comparison between EC3 and the original proposal for beam-columns in case of fire.” *Proceedings of the 5<sup>th</sup> European Conference on Steel and Composite Structures*, Graz, Austria.

- Tebedge, N., Alpsten, G., Tall, L. (1973) "Residual Stress Measurement by the Sectioning Method." *Proc. Soc. Experimental Stress Analysis*, 30, n°1.
- Villette M. (2004). "Assessment on the Behavior and Design of Beam-Columns and Proposal of New Formulations", *PhD Thesis*, University of Liège.